ISSN 2616-5767 Vol.7, Issue 3: 77-83, DOI: 10.25236/AJETS.2024.070311

Design and Optimization of a UHF High Gain Tag Antenna Based on HFSS

Hangwen Li*

School of Mechanical and Electronic Engineering, Wuhan University of Technology, Wuhan, 430070, China

**Corresponding author: lhw_lxg123123@whut.edu.cn*

Abstract: *As RFID technology advances, the demands on antenna performance also increase. In this paper, a UHF high-gain tag antenna with high gain, miniaturization and low profile is proposed, which achieves perfect impedance matching with Monza R6 chip by using an innovative F structure. The simulation analysis using performed with the HFSS software shows that the antenna has a normalized radiation gain of up to -4.7 dB, with a bandwidth of 47 MHz and overall dimensions of 40 mm × 40 mm × 3.2 mm. The miniaturized high-gain antenna proposed in this study has broad potential in the fields of future communications and the Internet of Things (IoT). It also provides valuable research insights for more efficient and reliable long-distance transmission.*

Keywords: *UHF RFID, Tag Antenna, Miniaturization, High Gain*

1. Introduction

Radio frequency identification technology (RFID) is a contactless identification technology that radio frequency communication. It identifies specific targets and reads and writes relevant via through radio waves without human intervention. With the rapid development of science and technology, the emergence and development of the Internet of Things and the current fifth-generation mobile communications (5G) are gradually transforming the entire world, and RFID technology is the realization of the Internet of Things, a key technology and an important cornerstone. From simple label identification to complex supply chain management[1], from intelligent medical networks[2] to embedded applications such as buildings[3], from track location tracking[4] to environmental security monitoring[5], RFID has gradually penetrated various fields. As the application of RFID technology is becoming more and more widespread, its development potential and application prospects have been highly concerned by global researchers and industry, It has become a key enabler for the development of Internet of Things (IoT) technology, which is the core technology for advancing the Internet of Everything (IoE)[6].

The current RFID technology allows the use of frequency bands that are divided into four bands: Low Frequency (LF: 125-135 kHz), High Frequency (HF: 13.56 MHz), Ultra High Frequency (UHF: 433 MHz, 860-960 MHz), and Microwave (MW: 2.45 GHz, 5.8 GHz). Among them, the UHF RFID system is low cost and has longer lifespan and lower energy consumption. With its technology's continuous development and application, UHF RFID has become an important identification system in logistics, ports, warehousing, and other fields. Nevertheless, UHF RFID technology's current promotion and application still faces many challenges. Analysis from the label side, the domestic problems faced include: label chip cost is high; limited label performance applications; in a changing electromagnetic environment, antennas must have enough robustness to ensure normal operation; shorter label antenna recognition distance and smaller gain; and label antenna miniaturization and integration complexity, etc.

Researchers have done a lot of related work in the UHF band. In pursuit of good metal resistance, Chiu and C.Y. et al. proposed a planar inverted F-based antenna structure[7] and Lee and Lim et al. proposed a planar inverted L antenna structure[8]. In order to achieve high gain and enhance the recognition distance, D. Kim and J. Yeo both proposed an embedded tag antenna using a metal reflective cavity to improve the actual gain, which reaches 7.1 dBi and obtains a superb three-fold recognition distance. Still, the metal cavity area has to be at least 0.43λ × 0.24λ and the embedding depth has to be 0.15λ[9]. In addition, the two researchers applied the rectangular patch-type AMC with offset through holes in the metal cavity of the embedded tag antenna. Based on the reflection characteristics of the AMC structure, the antenna was able to change from a single-band resonance to a dual-band resonance, enabling a recognition distance of up to 23.74 m[10]. However, metal cavities, AMC structures, etc, will

ISSN 2616-5767 Vol.7, Issue 3: 77-83, DOI: 10.25236/AJETS.2024.070311

expand the antenna size and increase the complexity of antenna design, bringing challenges to antenna miniaturization and high integration.

Therefore, based on the previous work, this paper focuses on designing a high-gain tag antenna, proposing a novel F-structure to improve its gain, enhancing the penetration ability while improving the recognition distance, effectively expanding the recognition range of the RFID system, thus greatly improving the recognition efficiency and shortening the recognition time, to enable its application in a wider range of fields. In this paper, the performance of this tag antenna is verified by HFSS simulation with its central operating frequency located at 922 MHz, bandwidth band of 887-934 MHz, and normalized radiation gain of -4.7 dB.

2. Tag Antenna Design

2.1 Design Process

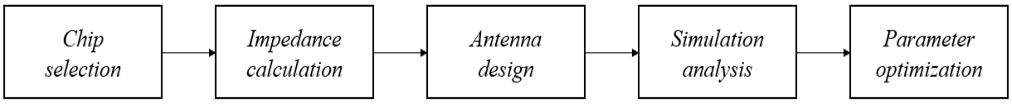

Figure 1: UHF RFID tag antenna design process.

For the design of the UHF RFID tag antenna, considering the complex impedance of the antenna, the design flow can be summarized in Figure 1.

(1) Chip selection: Different tag chip performance and usage requirements differ. The antenna design should be clear before actual application occasions and environment. Choose the appropriate tag chip model according to specific needs, and then determine the chip.

(2) Impedance calculation: At the same center frequency, the impedance of different chips is different. Before designing, we should check the equivalent parallel resistance and parallel capacitance of its RF port according to the chip datasheet. This way, we can calculate the input impedance of the labeled chip at a certain frequency point, as the conjugate impedance value of the antenna.

(3) Antenna design: Regarding the tag application occasions and environment, select the appropriate antenna type and material, and initially design the antenna’s specific shape, structure, and initial size so as to determine the range of its parameters.

(4) Simulation analysis: After completing the antenna shape design, the initial model can be constructed using the antenna modeling and simulation software. This allows for the optimization of antenna parameters and analysis of antenna performance.

(5) Parameter optimization: Using simulation software to scan and analyze the antenna parameters continuously adjusting the parameters to make the final design result meet the demand and realize the antenna design.

2.2 Chip selection and impedance calculation

A tag chip, as the unique electronic code of an RFID tag, can identify and recognize the object. In the UHF band, the domestic tag chip has some gaps in scale, industrialization, and performance compared to those from abroad. Currently, the more well-known RFID tag chip manufacturers are Impinj, Alien, TI, NXP, etc. In the country, Shanghai Kunrui, Zhihui Corelink and other companies also have some chip research and production.

Table 1 compares the performance of some commonly used label chips in the UHF band. From the table, it can be learned that the sensitivity of most of the chips is around -15 dBm, but the equivalent resistance is slightly different. In addition, for the selection of the label chip, it is necessary to meet the protocol standards, operating frequency, electrical performance and other conditions. Among them, the standard determines the operating frequency, the sensitivity relates to the read/write distance, the capacity determines the storage capacity, and the chip impedance is even more linked to impedance matching in the antenna design. Therefore, chip selection should be fully considered, and the most appropriate chip for the current application scenario and environment should be selected.

ISSN 2616-5767 Vol.7, Issue 3: 77-83, DOI: 10.25236/AJETS.2024.070311

Table 1: Comparison of the performance of some chips in the UHF band.

Manufacturer	**Chip**	**Read Sensitivity / dBm**	**Write Sensitivity / dBm**	**Equivalent Resistance / Ohm**	**Equivalent Capacitance / pF**
Alien	H3	-18	-14	1500	0.85
Alien	H4	-20.5	-17	1800	0.95
Impinj	Monza 4QT	-17.4	-14.6	1650	1.21
Impinj	Monza R6	-20	-16.7	1200	1.23
TI	RI_UHF_STRASP_08	-13	-9	380	2.8

According to the design requirements and performance comparison in this paper, the Monza R6 chip from Impinj was finally selected, and its shape is shown in Figure 2(a). Checking the chip datasheet shows that the chip's read sensitivity is -20 dBm while the write sensitivity is -16.7 dBm. The parallel equivalent resistance R_p is 1200 Ω, and the equivalent capacitance C_p is 1.23 pF. Then, the equivalent circuit model of the chip shown in Figure. 2(b) can be established.

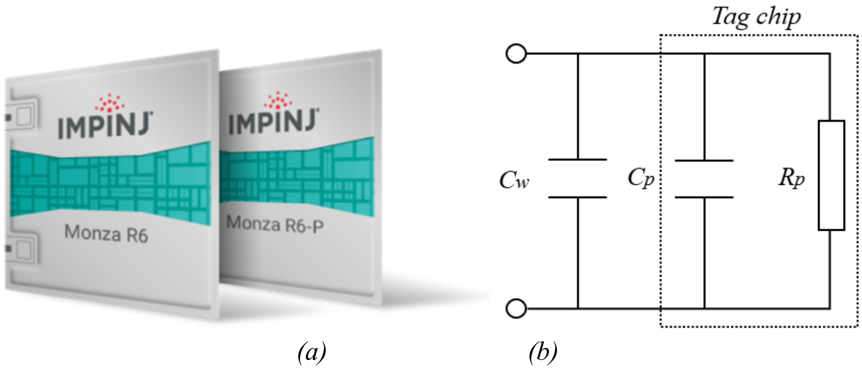

Figure 2: Chip model. (a) Chip shape. (b) Circuit model.

C_w is the parasitic capacitance generated when the chip is soldered, which is about 0.21pF. According to the equivalent circuit model in the ADS circuit simulation software, to create the corresponding simulation, 922 MHz is used as the center frequency. The calculation shows that the tag chip impedance is 11.86-j118.68 Ω. Based on the impedance matching theory, the tag antenna's input impedance should be 11.86+j118.69 Ω at the frequency.

2.3 Antenna structure design

This section describes the design of a tag antenna with an F structure, using specific parameters for the conductive medium and substrate material listed in Table 2. The antenna design is a symmetrical structure, as shown in Figure 3. The tag chip is at the center of the 40 mm × 40 mm × 3.2 mm antenna. To ensure effective impedance matching, four inverted F-shaped slits are etched on each end of the radiation patch in the chip, and a short-circuit wall is used for frequency and impedance adjustment.

Table 2: Textile characteristics.

Conductive textile	
Name	Copper
Conductivity	5.8×10^7 S/m
Thickness	0.035mm
Non-conductive textile	
Name	Rogers RO4003C
Thickness	3.13mm
Tanδ	0.0027
epsilon	3.55

ISSN 2616-5767 Vol.7, Issue 3: 77-83, DOI: 10.25236/AJETS.2024.070311

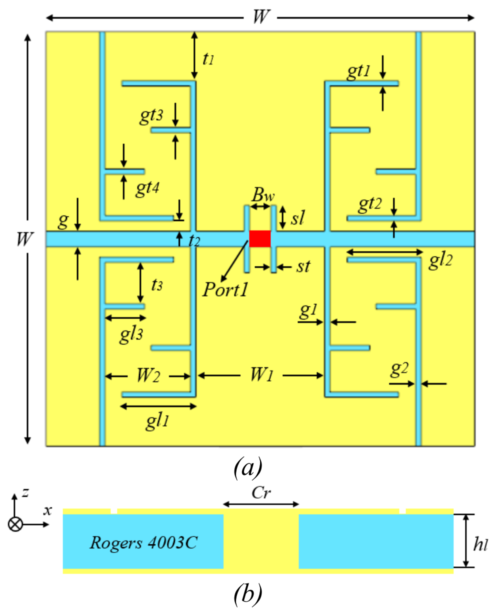

Figure 3: Tag antenna structure. (a) Top view. (b) Front view.

The antenna modeling and simulation were performed using the HFSS 2021 R2 software. Although the antenna structure introduces more adjustable variables, the simulation results provide some reference value for designing other antennas. The HFSS port model Port1 simulates the conjugate input impedance of the chip at 922 MHz center frequency, with a value of 12+j119 Ω. Table 3 shows the overall dimensions of the final tag antenna after optimization.

Table 3: Tag antenna parameters.

Parameters	Size(mm)	Parameters	Size(mm)
t_1	4	W	40
t_2	1	W_1	12
t_3	4	W_2	8
gt_1	0.5	B_w	2
gt_2	0.5	s_l	5
gt_3	0.5	s_t	0.5
gl_1	6.9	g_1	0.5
gl_2	6.9	g_2	0.5
gl_3	3.7	h_l	3.13
g	1.5		

3. Simulation Analysis and Optimization

3.1 Simulation analysis

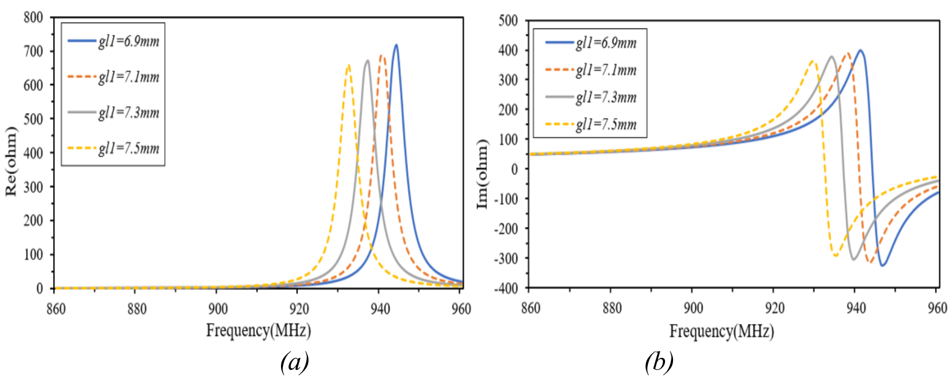

Figure 4: Impedance effects of gl_1. (a) Resistence effects. (b) Reactance effects.

ISSN 2616-5767 Vol.7, Issue 3: 77-83, DOI: 10.25236/AJETS.2024.070311

Intending to improve its overall performance, this section discusses and optimizes the etched F-shaped slit structure to explore the radiation performance and impedance-matching relationship of the antenna. The antenna center operating frequency selected is 922 MHz. The relevant parameters were optimized using the HFSS software, and the changes in antenna impedance were studied according to the law, followed by the corresponding adjustments.

The parameter gl_1, which controls the F-shaped slit, was analyzed first. Figure 4 demonstrates the change in antenna impedance when gl_1 is increased from 6.9 mm to 7.5 mm. The parameter scans are performed in steps of 0.2 mm because adjacent length variations have a small effect on impedance. The simulation results show that as gl_1 increases, the peak frequency of the antenna impedance gradually shifts to the left, causing the resistance and reactance values of the antenna to increase. The changes are more pronounced for smaller parameter values, while at the same frequency point, the antenna's impedance decreases. Accordingly, it can be seen that controlling the size of gl_1 can adjust the impedance-matching frequency of the tag antenna and at the same time, fine-tuning the size of the impedance at a certain frequency point to realize impedance matching.

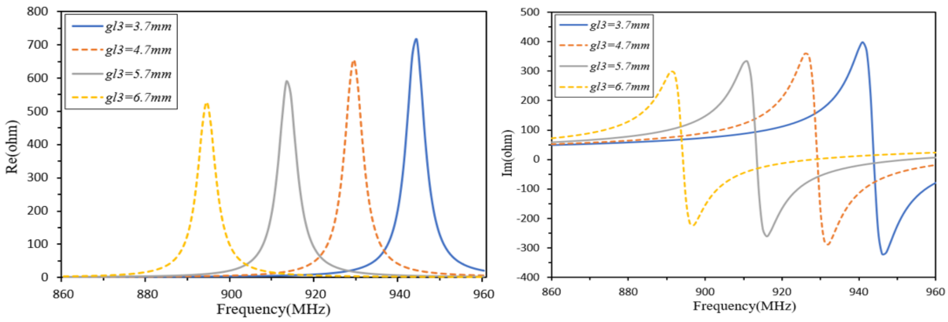

(a) *(b)*

Figure 5: Impedance effects of gl_3. (a) Resistance effects. (b) Reactance effects.

Meanwhile, the parameter gl_3, which controls the length of the transverse slit at the back end of the F-shaped slit, was analyzed. Figure 5 demonstrates the variation of the antenna impedance as gl_3 is increased from 3.7 mm to 6.7 mm in steps of 1 mm. The simulation results show that as gl_3 increases, the peak frequency of the antenna impedance shifts to the left and decreases. At the same frequency point, the resistance and reactance values of the antenna vary more and tend to increase. Accordingly, it can be seen that controlling the size of gl_3 can effectively adjust the impedance-matching frequency of the tag antenna to adjust to the desired operating frequency point.

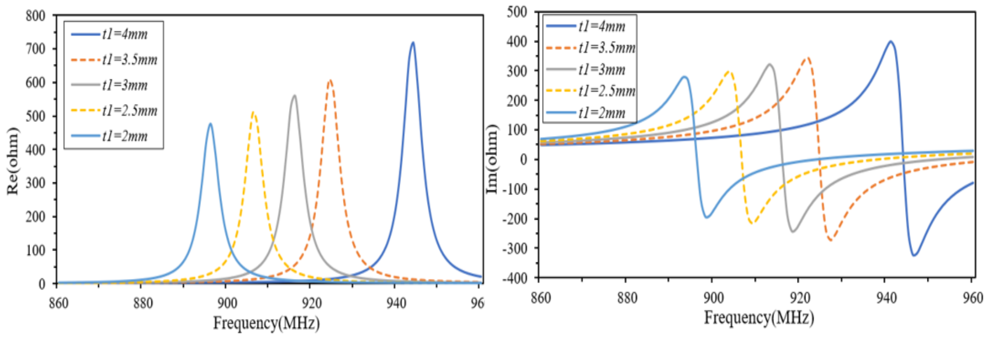

(a) *(b)*

Figure 6: Impedance effects of t_1. (a) Resistance effects. (b) Reactance effects.

Additionally, we analyzed the parameter t_1, which controls the length of the vertical slit of the F-shaped slit. Figure 6 shows impedance variation as t_1 increases from 2 mm to 4 mm with a step increase of 0.5 mm. The simulation results show that as t_1 increases, the peak frequency of the antenna impedance shifts to the right and changes more significantly. The antenna's resistance and reactance values tend to decrease at the same frequency point. Accordingly, it can be seen that controlling the size of t_1 can effectively adjust the impedance-matching frequency of the tag antenna. This adjustment can be made to reach the desired operating frequency by coupling with other parameters.

ISSN 2616-5767 Vol.7, Issue 3: 77-83, DOI: 10.25236/AJETS.2024.070311

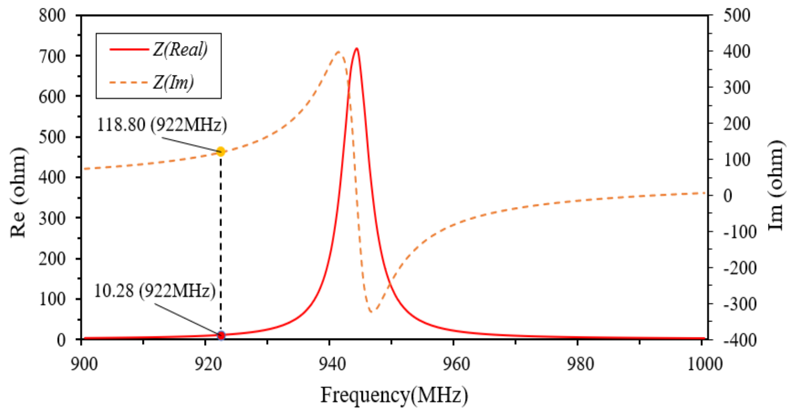

Figure 7: Impedance of the optimized antenna.

In summary, the F-shaped slit's impedance matching frequency can be achieved by controlling its horizontal slit length parameters, gl_1 and gl_3, and other relevant parameters to operate the antenna at the desired frequency point. Additionally, the vertical slit length parameter, t_1, and other relevant parameters can be adjusted to fine-tune the impedance size, resulting in improved impedance matching with the label chip.

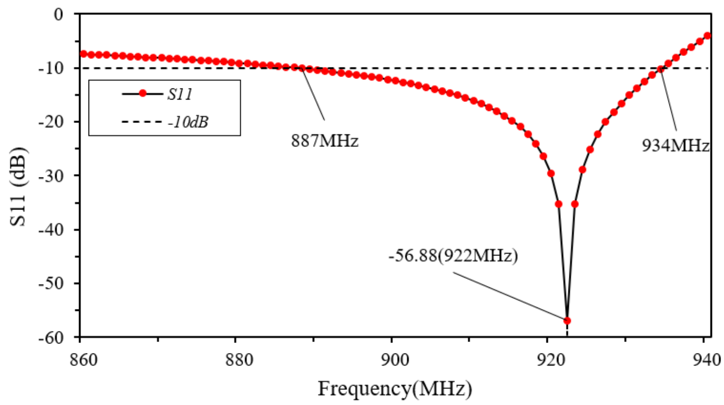

Figure 8: S_{11} curve of the optimized antenna.

3.2 Parameter optimization

After analyzing the study, some antenna parameters were optimized to achieve impedance matching and improve overall antenna performance. Figure 7 shows the antenna impedance after optimization from 900 MHz to 1 GHz. The figure shows that the antenna impedance value at 922 MHz is 10.28+j118.8 Ω, while the chip impedance is 11.86-j118.68 Ω. These values can be approximated to achieve conjugate matching. Meanwhile, the return loss S_{11} can be used to describe the degree of impedance matching between the tag antenna and the chip. The S_{11} curve of the optimized antenna is shown in Figure 8.

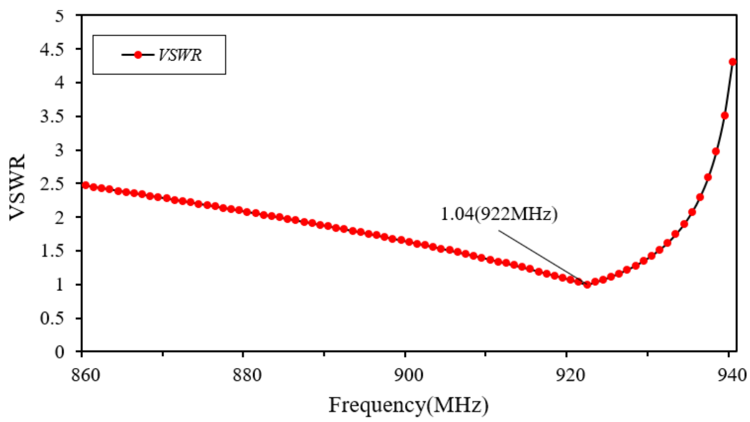

Figure 9: VSWR curve of the optimized antenna.

ISSN 2616-5767 Vol.7, Issue 3: 77-83, DOI: 10.25236/AJETS.2024.070311

Figure 8 shows that the tag antenna has a return loss of approximately -56.88 dB at the resonance point of 922 MHz, with a bandwidth of up to 47MHz. Additionally, Figure 9 indicates a voltage standing wave ratio of 1.04 ($1 < VSWR < 1.5$), suggesting that almost 99% of the capacity can be radiated, meeting the design requirements. Figure 10 shows the directional gain plot of the antenna. It is evident that the antenna has an omnidirectional characteristic, with a normalized radiation gain of approximately -4.7 dB. Additionally, the directional plot in the E-plane is symmetric at a certain radiation angle, further demonstrating the antenna's omnidirectional characteristic.

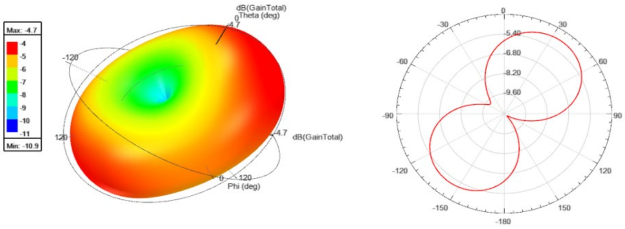

(a) *(b)*

Figure 10: Radiation direction pattern of the antenna. (a) 3D pattern (b) Simulated pattern

4. Conclusions

In this paper, a high-gain UHF tag antenna with a novel F-structure is proposed to achieve perfect impedance matching of RFID chips at a central operating frequency of 922 MHz. Optimized by HFSS simulation software, the tag antenna shows excellent performance metrics. Its maximum normalized radiation gain is -4.7 dB, with a return loss of -56.88 dB at 922 MHz and a bandwidth of up to 47 MHz. These results significantly enhance the penetration capability and detection range of the system. Therefore, the antenna can provide reliable connection quality for IoT devices, maintaining communication continuity and accuracy even over long distances or in obstructed conditions. In conclusion, this new F-structure UHF tag antenna shows great potential and application value in modern communication systems with its excellent performance and adaptability to future technology trends. As 5G and IoT technologies continue to advance, the design concepts and technical details of this antenna will bring more innovation and breakthroughs to the communications field.

References

[1] Zhu, X., Mukhopadhyay, S. K., & Kurata, H. (2012). A review of RFID technology and its managerial applications in different industries. Journal of Engineering and Technology Management, 29(1), 152-167.

[2] Taylor, P. S., & Batchelor, J. C. (2019). Finger-worn UHF far-field RFID tag antenna. IEEE Antennas and Wireless Propagation Letters, 18(12), 2513-2517.

[3] Jeong, S. H., & Son, H. W. (2011). UHF RFID tag antenna for embedded use in a concrete floor. IEEE Antennas and Wireless Propagation Letters, 10, 1158-1161.

[4] D'Avella, S., Unetti, M., & Tripicchio, P. (2022). RFID Gazebo-based simulator with RSSI and phase signals for UHF tags localization and tracking. IEEE Access, 10, 22150-22160.

[5] Yang, L., Zhang, R., Staiculescu, D., Wong, C. P., & Tentzeris, M. M. (2009). A novel conformal RFID-enabled module utilizing inkjet-printed antennas and carbon nanotubes for gas-detection applications. IEEE Antennas and Wireless Propagation Letters, 8, 653-656.

[6] Jia, X., Feng, Q., Fan, T., & Lei, Q. (2012, April). RFID technology and its applications in Internet of Things (IoT). In 2012 2nd international conference on consumer electronics, communications and networks (CECNet) (pp. 1282-1285). IEEE.

[7] Chiu, C. Y., Shum, K. M., & Chan, C. H. (2007). A tunable via-patch loaded PIFA with size reduction. IEEE transactions on antennas and propagation, 55(1), 65-71.

[8] Lee, Y. H., Lim, E. H., Bong, F. L., & Chung, B. K. (2020). Loop-fed planar inverted-L antennas (PILAs) for omnidirectional UHF on-metal tag design. IEEE Transactions on Antennas and Propagation, 68(8), 5864-5871.

[9] Kim, D., & Yeo, J. (2010). A passive RFID tag antenna installed in a recessed cavity in a metallic platform. IEEE Transactions on Antennas and Propagation, 58(12), 3814-3820.

[10] Kim, D., & Yeo, J. (2008). Low-profile RFID tag antenna using compact AMC substrate for metallic objects. IEEE Antennas and Wireless Propagation Letters, 7, 718-720.